European Polymer Journal 47 (2011) 130–138

Contents lists available at ScienceDirect

European Polymer Journal

journal homepage: www.elsevier.com/locate/europolj

Macromolecular Nanotechnology

Patterns of surface immobilized block copolymer vesicle nanoreactors

Qi Chen, G. Wilhelmina de Groot, Holger Schönherr *, G. Julius Vancso *

Department of Materials Science and Technology of Polymers, University of Twente, MESA+ Institute for Nanotechnology, Postbus 217, 7500 AE Enschede, The Netherlands

ARTICLE INFO

Article history:
Received 3 September 2010
Received in revised form 19 October 2010
Accepted 9 November 2010
Available online 7 December 2010

Keywords:
Block copolymer vesicles
Soft lithography
Micro-molding in capillaries
Enzyme and substrates

ABSTRACT

The immobilization and positioning of ultra small reaction vessels on solid supports open new pathways in applications such as lab-on-a-chip, sensors, microanalyses and microreactors. In our work block copolymer vesicles made from polystyrene-*block*-polyacrylic acid (PS-*b*-PAA) were immobilized from aqueous medium onto 3-amino propyl trimethoxysilane functionalized silicon surfaces exploiting electrostatic interactions. The immobilization of the vesicles was investigated by Fourier transform infrared (FTIR) spectroscopy, as well as fluorescence optical and atomic force microscopy (AFM). In addition, the influence of pH and ionic strength on the surface coverage of vesicles bound to the surface was elucidated. Finally micro-molding in capillaries (MIMIC) was utilized to create line patterns of the vesicles containing the enzyme trypsin and the fluorogenic substrate rhodamine 110 bisamide. The selective positioning of vesicle nanoreactors in conjunction with electrostatic immobilization serves as a proof of principle for potential applications in real-time observation of confined chemical reaction inside vesicles as nanocontainers and for the fabrication of integrated microarray systems.

1. Introduction

Miniaturized integrated systems with large numbers of isolated or inter-connected functional units are promising targets for applications in the fields of bio-analysis and biosensing [1,2]. Owing to their unique structure vesicles comprised e.g., of lipids or block copolymers (BCP, so-called "polymersomes") possess typical diameters of several tens to hundreds of nanometers and are considered to be attractive candidates for ultra-small individual units in an integrated microarray system. The closed membrane of the vesicles isolates the interior from outside space and can provide a microenvironment different from the bulk [3]. Furthermore, the architecture of these vesicles, including overall dimensions, membrane thicknesses and structures, can be precisely tuned and various substances, such as biomolecules or fluorescent probes, have been successfully encapsulated in the vesicles' interior. Compared to their lipid analogues, BCP vesicles exhibit considerably enhanced mechanical properties and hence robustness. Integration of polymersomes as individual units with ultrasmall internal volume in a microarray system may not only be useful to address the dynamic behavior of enzymes and DNA [4], but may also find application in protein chips [5,6], sensors [7,8], microanalysis [9] and micro-reactors [10,11].

To date different methodologies were applied to immobilize BCP or lipid vesicles on solid supports. These strategies utilized electrostatic interactions, receptor-ligand binding or covalent coupling [4]. In studies carried out by Li et al. [12,13] vesicles formed with Pluronic L121 (PEO5-PPO68-PEO5) triblock copolymers were immobilized on negatively charged surfaces via negatively charged polyelectrolytes in combination with Mg^{2+} ions. In another example, Stamou et al. [14,15] immobilized lipid vesicles on micropatterned supports exploiting the streptavidin–biotin ligand-receptor

* Corresponding authors. Present address: University of Siegen, Department of Physical Chemistry I, Adolf-Reichwein-Str. 2, 57076 Siegen, Germany. Tel.: +49 (0) 271 740 2806; fax: +49 (0) 271 740 2805 (H. Schönherr).

E-mail addresses: schoenherr@chemie.uni-siegen.de (H. Schönherr), g.j.vancso@tnw.utwente.nl (G. Julius Vancso).

0014-3057/$ - see front matter © 2010 Elsevier Ltd. All rights reserved.
doi:10.1016/j.eurpolymj.2010.11.005

pair and investigated biochemical reactions in these nanoreactors.

In general, soft lithography techniques, e.g., microcontact printing (μCP) and micro-molding in capillaries (MIMIC) [16], facilitate the arraying or patterning of vesicles onto surfaces under common laboratory conditions. However, the interaction between the vesicles and the substrate remains the key issue in the process [4]. Utilizing electrostatic interactions, Mahajan et al. [17] immobilized 1,2-bis (tricosa-10,12-diynoyl)-sn-glycero-3-phosphocholine (DC8, 9PC) lipid vesicles in a patterned fashion on glass substrates using both μCP and MIMIC. The latter soft lithographic technique was also used by Baek et al. [18] to fabricate patterns of covalently immobilized poly(diacetylene) vesicles for future use in sensor and optical applications [19].

In our previous studies, the enzyme-catalyzed hydrolyses of fluorogenic substrates were elucidated *inside* PS-*b*-PAA vesicle nanoreactors [20,21]. A marked increase in enzyme activity and reactions rates was observed for reactions inside vesicles with decreasing inner diameter. These results agree with data reported by other research groups [15,22,23]. In order to observe enzymatic reactions that take place inside individual nanoreactors with precisely defined inner volume in real-time using microscopy techniques, it is highly desirable to immobilize these nanoreactors in a controllable way onto selective regions of solid surfaces.

In this work a versatile approach to immobilize PS_{139}-*b*-PAA_{17} vesicle nanoreactors containing the enzyme trypsin and a fluorogenic substrate onto 3-aminopropyl trimethoxysilane-functionalized silicon/silicon oxide surfaces based on electrostatic interaction was explored (Scheme 1). Combining electrostatic interactions and soft lithography line patterns of the vesicles were created, which serve as a prerequisite for the dynamic study of enzymatic reactions inside these nanoreactors and a potential way for preparing future microarray systems utilizing these vesicles as functional elements.

2. Materials and methods

2.1. Materials

PS_{139}-*b*-PAA_{17} (the subscripts denote the number of repeat units for respective blocks) were purchased from Polymer Source Inc. (Dorval, Canada). 3-Aminopropyl trimethoxysilane (APTMS), sodium hydroxide (0.1 M), hydrochloric acid (0.1 M) and bovine pancreas trypsin were purchased from Sigma–Aldrich, Inc. (St. Louis, MO, USA). The fluorogenic substrate rhodamine 110 bis-(benzyloxycarbonyl-L-arginine amide) dihydrochloride (R110-Arg2) was purchased from Molecular Probes/Invitrogen Co. (Carlsbad, CA, USA). Buffer solution containing sodium chloride and sodium hydrogen phosphate and sodium dihydrogen phosphate were purchased from B. Braun

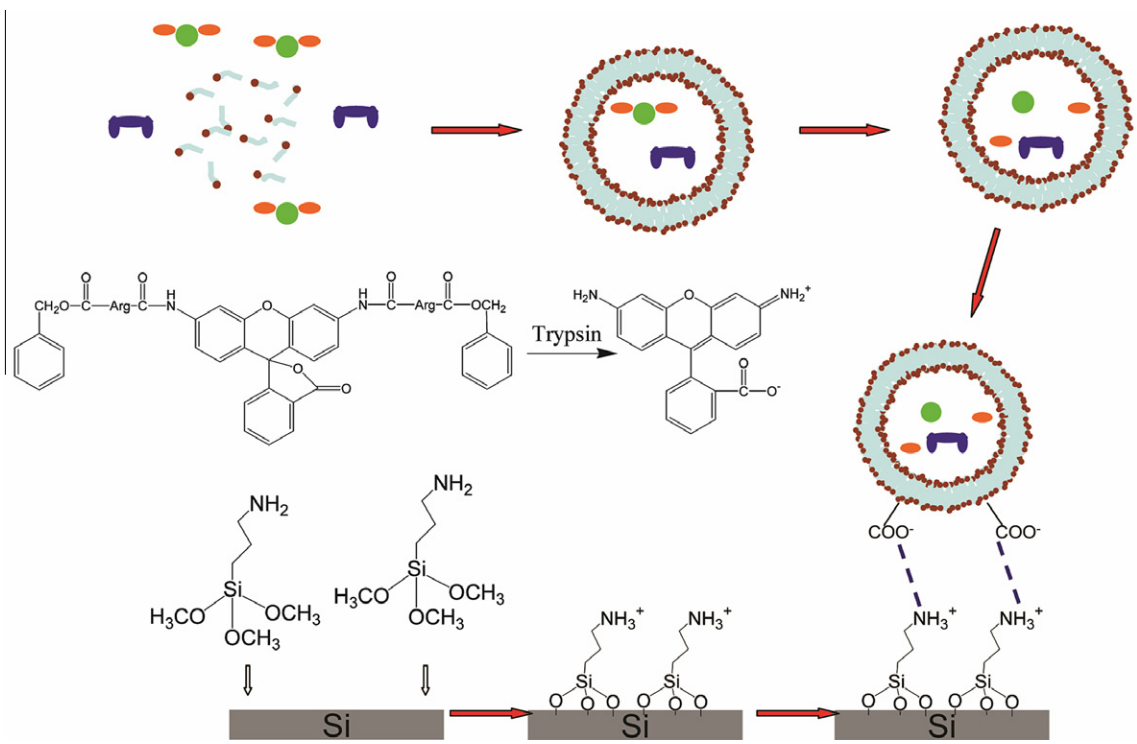

Scheme 1. Schematic of the vesicle immobilization strategy. Vesicles were formed by mixing an aqueous solution of trypsin ( ) and R110-Arg_2 ( ) with a PS-*b*-PAA solution in THF. Silicon (or glass) substrates were treated with APTMS. On these amino-terminated substrates PS-*b*-PAA vesicles were immobilized via electrostatic interactions between the positively charged amino groups of the surface and the negatively charged carboxylic acid groups of the polymersome corona. The fluorescent probe R110 ( ) was formed as the product of the enzymatic reaction, as shown in the reaction equation.

Melsungen AG (Melsungen, Germany). Tetrahydrofuran (THF) (AR grade) was purchased from Biosolve B. V. (Valkenswaard, the Netherlands). Milli-Q water was produced with a Millipore Synergy system (Billerica, MA, USA). All chemicals were used as received.

2.2. Preparation of PS-b-PAA vesicles

PS-*b*-PAA vesicles were prepared by first dissolving the polymer in THF (V = 0.5 mL) with initial concentrations of 2 wt.%, then adding Milli-Q water (or an aqueous solution containing the enzyme (c = 0.05 μM) and substrate (c = 12.8 μM)) as a precipitant into the polymer solution until a given water percentage (50 vol.%) was reached, while the entire system was under vigorous stirring using a magnetic stirring bar at ~600 rpm. An excess amount of water (V = 5 mL) was then added to "freeze" the morphology of the aggregates. Enzymes and substrates were encapsulated in the vesicles by dissolving both trypsin and R110-Arg_2 in water followed by immediate mixing. After stirring for overnight, the solution mixture was subjected to dialysis for 72 h to remove any residual organic solvent as well as unencapsulated enzymes and substrates. Dialysis was carried out using Spectra/Por 7 dialysis tubing from Spectrum Europe B.V. (Breda, the Netherlands) with a molecular weight cut off of 12–14 kD.

The size of the PS-*b*-PAA vesicles was determined with a Malvern Zeta-sizer 4000 (Malvern Corp., Malvern, UK) at 25 °C using a laser wavelength of 633 nm and a scattering angle of 90°. The CONTIN method was applied for data processing [24]. The size, count rate and poly-dispersity index (PDI) of the vesicles were determined.

2.3. Immobilization of vesicles onto surfaces

Silicon and glass substrates of approximately 1 cm × 1 cm were used in the immobilization experiments. Substrates were first cleaned with piranha solution (3:1 (v:v) mixture of concentrated sulfuric acid and 30% hydrogen peroxide) to remove organic impurities [*Caution! Piranha solution should be handled with extreme caution; it has been reported to detonate unexpectedly.*], subsequently silanized by immersion into a APTMS solution in toluene (10 mM) for 8 h. The APTMS-coated substrates were subsequently rinsed with toluene and dried under nitrogen. The immobilization of the vesicles was carried out by immersing the substrates into vesicle solutions (10 times diluted as prepared with the addition of NaOH or HCl and/or buffer solution to have various pHs and ionic strengths) for 2 h. Afterwards the samples were taken out and rinsed extensively with Milli-Q water and dried under nitrogen flow.

2.4. Characterization of surface-immobilized vesicles

AFM images were obtained under ambient conditions in tapping mode with a NanoScope IIIa multimode atomic force microscope (Digital Instruments/Veeco, Santa Barbara, CA, USA) using silicon cantilevers with resonance frequencies of 200–500 kHz (type PPP-NCH-W, Nanosensors, Wetzlar, Germany) and a J-scanner (Digital Instruments/Veeco).

Transmission mode FTIR spectra were obtained using a BIO-RAD model FTS575C FTIR spectrometer (Bio-rad Laboratories, Inc., Hercules, CA, USA) equipped with a liquid nitrogen cooled cryogenic mercury cadmium telluride (MCT) detector. Background spectra were obtained using cleaned silicon substrates.

Fluorescence microscopy images were obtained on an Olympus inverted microscope IX71 (Olympus, Tokyo, Japan) equipped with a U-RFL-T mercury burner as the light source and a digital camera for image acquisition. Blue excitation (450 nm < λ < 480 nm) and green emission light (λ > 515 nm) were properly filtered using a U-MWG Olympus filter tube (Olympus, Tokyo, Japan).

2.5. Patterning of vesicles onto surfaces using MIMIC

Patterning of PS-*b*-PAA vesicles was carried out using PDMS stamps with channels of 16 μm and a height of 20 μm. The PDMS stamps were rendered hydrophilic with O_2 plasma treatment using an ozone reactor (UV PRS-100, Photonic Research Systems, Salford, UK). Typical treatment condition were: UV emission at 185 nm (1.5 mW cm^{-2}); concentration of ozone 55 ppm; 1 h of irradiation. Afterwards the PDMS stamps were placed onto glass substrates cleaned with piranha solution (*vide supra*). A solution containing trypsin and R110-Arg_2 loaded vesicles (prepared from solutions of 2 wt.% PS-*b*-PAA in THF with 50% water content) was placed at the channel opening at the edge of the stamp. Filling of the channels immediately took place as a result of capillary force. The process was recorded *in situ* using optical microscopy (Olympus IX71, Olympus, Tokyo, Japan). After drying at room temperature the stamps were removed and the samples were rinsed extensively with Milli-Q water.

3. Results and discussion

The fabrication of patterned arrays of ultrasmall volume reaction vessels exploiting polymersomes is based on the establishment of a reproducible strategy to firmly immobilize reactant-loaded PS-*b*-PAA vesicles on solid supports. Thus, following the assembly of the BCP into polymersomes and the loading of reactants, the immobilization via electrostatic interactions was investigated in detail, in particular the effect of pH and ionic strength.

Finally, the micro-patterning by soft lithography will be discussed.

3.1. Formation of trypsin and R110-Arg_2 containing PS-b-PAA vesicles

BCP vesicles were prepared by mixing a solution of PS-*b*-PAA in THF with water as described in previous studies [20,25]. Trypsin and R110-Arg_2 dissolved in water can be encapsulated in this formation step. After a specific water content was reached, an excess amount (5× diluted) of water was added into the solution to quench or "freeze" the morphology of the aggregates. Subsequent dialysis of the vesicle mixture against water allowed the removal of THF, as well as non-encapsulated compounds. According

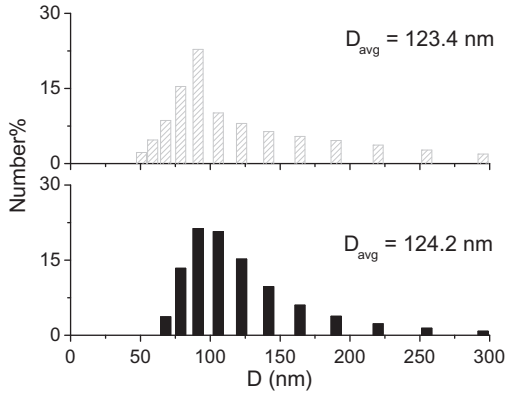

Fig. 1. Size distribution histogram of trypsin and R110-Arg_2 containing PS-*b*-PAA vesicles (grey) and empty vesicles (black). Preparation conditions for two vesicle samples are the same. D_{avg} refers to the arithmetic mean diameter. In the case of enzyme and substrate containing vesicles, trypsin (C = 0.05 μM) and R110-Arg_2 (C = 12.8 μM) solution instead of pure water is added into the polymer solution.

to dynamic light scattering (DLS) results, the presence of trypsin and R110-Arg_2 did not affect the average size, as well as the size distribution of vesicles, shown in Fig. 1.

3.2. Investigation on the electrostatic immobilization of PS-*b*-PAA vesicles on NH_2-terminated surfaces

In order to facilitate the electrostatic interactions between the PS-*b*-PAA vesicles and the substrates, surface silanization was carried out to introduce amino groups onto the silicon surface (see Scheme 1). The NH_2-terminated substrates were then immersed into PS-*b*-PAA vesicles solution (pH 7.4, I = 50 mM) for 2 h, followed by immersion into pure water and extensive rinsing to remove physisorbed vesicles. The samples were characterized with FTIR spectroscopy. In addition, a control experiment with unmodified silicon substrates was carried out. Selected regions of FTIR spectra are shown in Fig. 2 for the NH_2-terminated substrates as well as the control sample.

The band assignments as well as the peak wavenumbers of the major absorption bands in the spectra of PS-*b*-PAA are indicated in Fig. 2 [26]. Clear differences were observed in the FTIR spectra of the two samples. In the spectrum of samples prepared on NH_2-terminated substrates the major absorption bands of PS-*b*-PAA were clearly discernible. By contrast, for the control sample the spectra did not provide evidence for the presence of PS-*b*-PAA.

These data are fully supported by atomic force and fluorescence microscopy analyses (Fig. 3). In particular the presence of *intact* vesicles was concluded from the AFM micrographs. PS-*b*-PAA vesicles deposited on NH_2-terminated silicon surface were imaged with tapping mode (TM) AFM in air, as shown in Fig. 3e. The vesicles retained their spherical shapes and arranged in a random close-packed manner on the NH_2 surface. In a large scan area (50 μm × 50 μm) no vesicles were found on the surface of the control sample (Fig. 3f inset).

All microscopic measurements, as well as the FTIR spectroscopy results, pointed to the conclusion that a much stronger affinity exists between PS-*b*-PAA vesicles and NH_2-terminated surfaces as compared to vesicles and non-silanized surfaces. This difference is attributed to the electrostatic interaction between the negatively charged carboxylic acid groups present on the vesicles and the positively charged amino groups (pK_a 10–11) [27] on the surface under the experimental conditions. By contrast, such interactions are virtually absent for silicon surfaces (pK_a 1.7–3.5) [28].

In order to determine the amount of polymer adsorbed on the surfaces from the FTIR spectroscopic data, measurements on reference thin films were carried out. For this purpose, thin PS-*b*-PAA reference films were prepared by spin-coating the polymer from THF solution onto Si with different spinning speeds and polymer concentrations. The thicknesses of the obtained polymer thin films were determined with ellipsometry. Subsequently, the films were characterized using FTIR spectroscopy.

The characteristic absorption of PS-*b*-PAA at 3026 cm^{-1} (assigned to the vibration of the aromatic ring of PS) is shown in Fig. 4 for films with different thicknesses. The absorbance of this band was integrated and plotted against the film thickness, as shown in the inset. A linear relationship of film thickness (t) and absorbance (Abs) was observed, which is described by: $t = 1014 \cdot Abs + 5.3$ (R^2 = 0.95).

3.3. Influence of pH and ionic strength on the electrostatic immobilization

In order to prove that the PS-*b*-PAA vesicles are immobilized at the NH_2-terminated surface via electrostatic interactions, immobilization experiments were carried out at different pH values. The ionization of the vesicle surface and the substrate surface is sensitively related to the pH of the

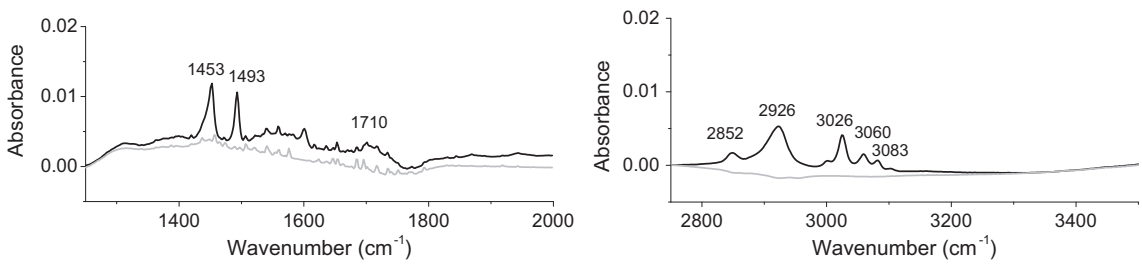

Fig. 2. FTIR spectra of PS-*b*-PAA vesicles deposited onto silicon substrates with (black) and without (grey) surface silanization. The band positions of the characteristic vibration bands of PS-*b*-PAA are indicated in the graph (the band assignment is shown in footnote [26]).

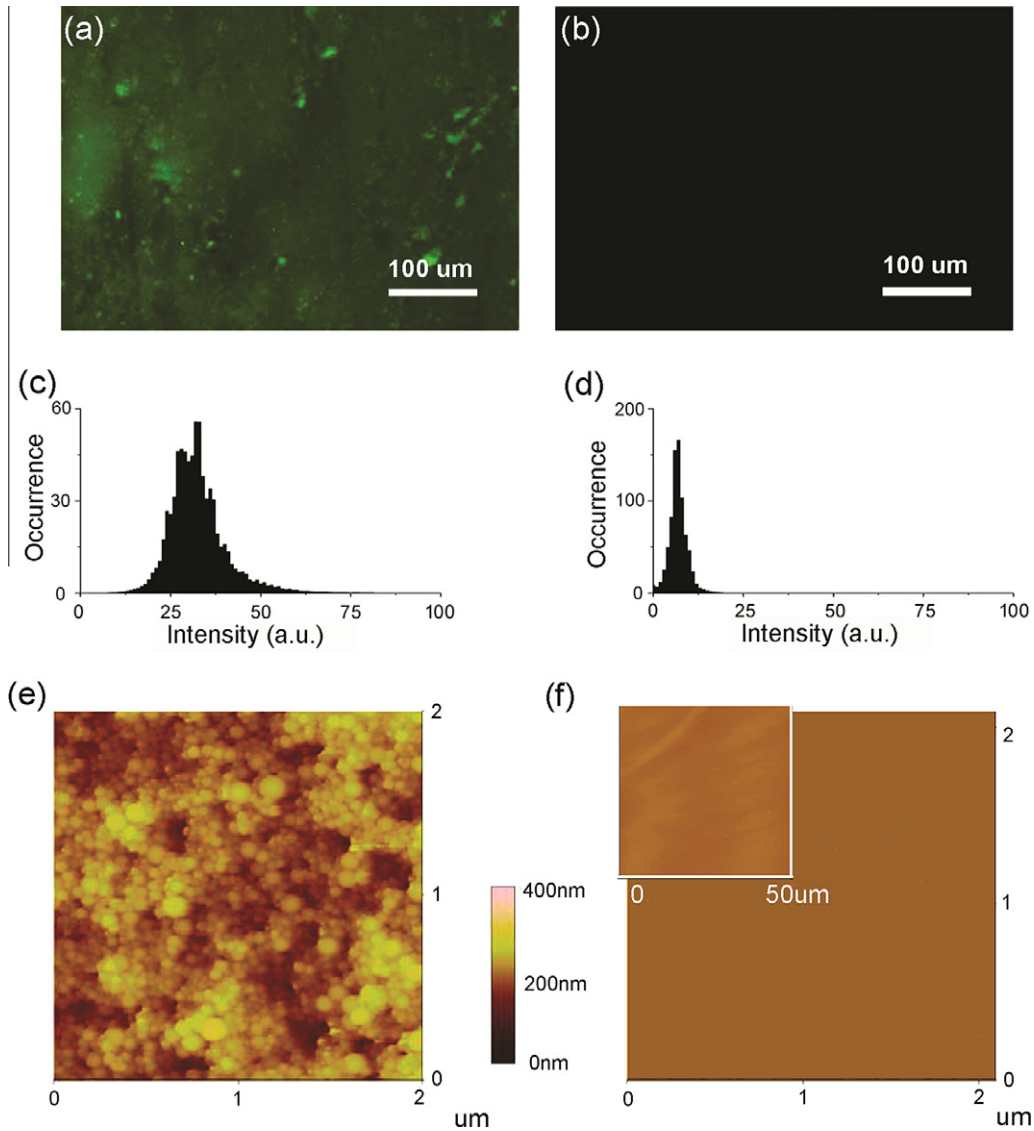

Fig. 3. Top: Fluorescence microscopy images of PS-*b*-PAA vesicles preloaded with rhodamine 110 on (a) NH_2-SiO_2 and (b) bare glass substrates and (c), (d) the corresponding intensity histograms of the fluorescence images. Bottom: TM-AFM images of PS-*b*-PAA vesicles deposited on (e) NH_2-Si and (f) Si substrates. The inset shows a zoom-out image with scan size of 50 μm.

environment. By varying the pH, it is possible to change the degree of ionization of one or both of the opposite charges, thus enhancing or weakening the electrostatic interaction between the vesicles and the surfaces. In our experiments standard sodium hydroxide (or hydrochloric acid) solution (0.1 M) was added to the vesicle solution to modify the pH. Sodium chloride was added to keep the ionic strength of the solution constant. NH_2-terminated silicon substrates were then immersed into the vesicle solutions, followed by rinsing with water of the corresponding pH. The samples were subsequently characterized with FTIR spectroscopy. The absorption peaks at 3026 cm^{-1} of different samples (I = 14 mM) are shown in Fig. 5a.

The FTIR spectra for samples (I = 14 mM) prepared at different pH showed different values for the integrated absorption, indicating that different amounts of polymer (vesicles) were adsorbed onto the surfaces under different pHs. The spectra were integrated and the absorption was converted to thickness according to the calibration curve obtained from the inset of Fig. 3. This is further converted into the number of vesicles per unit area [29], assuming that the size of the vesicles is homogenous on the surface. The result is shown as a function of pH in Fig. 5b (squares). As can be seen in the graph, the amount of polymer adsorbed onto the surfaces was low at both low and high pH and reached a maximum at around neutral pH. This indicates the interaction between the vesicles and the surfaces is of electrostatic nature: At a pH below the pK_a of both acrylic acid (4.25)[30] and APTMS (10–11), the carboxylic acid groups presented on the surface of the vesicles are protonated, thus are not negatively charged while the amine groups on the substrates are positively charged; at

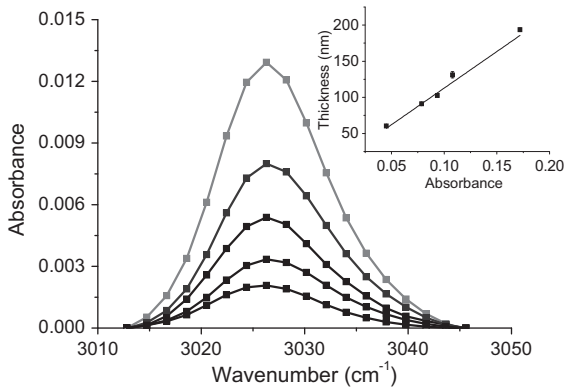

Fig. 4. Section of FTIR spectra showing the characteristic absorption peak of PS-*b*-PAA at 3026 cm^{-1} for different polymer film thicknesses. The inset shows a plot of the film thickness vs. the integrated absorption at 3026 cm^{-1} with a linear least squares fit (represented by the solid line) to the data.

pH above the pK_a of both primary amine and acrylic acid, the amine groups on the substrates are de-protonated, therefore losing their positive charges, yet the carboxylic acid groups on the polymer chains are negatively charged. In both cases, the electrostatic interaction is less pronounced since one of the opposite charges is absent. At neutral pH, as acrylic acid is above its pK_a and the amine is below its pK_a, both functional groups are charged and these facilitate the interaction between the opposite charges. All three scenarios are also schematically shown in Fig. 5b.

The strength of electrostatic interaction is also related to the ionic strength of the solution. To study the influence of solution ionic strength on the immobilization process, additional salt (NaCl) was added in the solutions with a different pH. As can be seen in Fig. 5b (circles), experiments with higher ionic strength (I = 100 mM) clearly showed higher amounts of vesicles adsorbed onto the surfaces under all pH conditions. This is primarily the result of the screening of surface charges. The Debye screening length, which is the scale over which mobile charge carriers screen out electric fields in an electrolyte or in a colloid system, depends on the salt concentration. With increasing salt concentration, the Debye length decreases, reducing the repulsion between the vesicles [31]. The attraction between the vesicles due to van der Waals interaction is essentially the same, according to the DLVO theory [32]. This would result in larger number of vesicles immobilized onto the surface at increased ionic strength. In our experiments with the addition of salt above 35 mM full coverage (in 10 × 10 μm^2) of vesicles was achieved at neutral pH. (Fig. 6g and h).

The morphology of the vesicles immobilized onto NH_2-terminated silicon at different pH, as well as ionic strengths was analyzed with AFM (Fig. 6). It is clearly seen that at low and high pH fewer vesicles were immobilized onto the substrates in a 10 μm × 10 μm scan area than at neutral pH. It should be noted that the size variation of the vesicles in different images was primarily due to the convolution of the AFM probes as section analysis showed that the height of the vesicles was essentially the same. Based on the conversion mentioned above, the coverage of vesicles was determined by FTIR spectroscopy. A fully covered surface corresponded to ~50 vesicles per μm^2 or a 62 nm film thickness. AFM bearing analysis was used to determine the surface coverage of vesicles on the image area. In bearing analysis, a histogram of the distribution of surface height over the sample surface was constructed based on the occurrence of pixels at a specific height. The bearing area was also calculated for each specific height and was used here for the determination of surface coverage. According to AFM bearing analysis (n = 5 images) the surface coverages of vesicles in Fig. 6a–c are 16.5 ± 1.2% (pH 4.2, I = 14 mM), 37.3 ± 3.2% (pH 7.8, I = 14 mM) and 12.8 ± 1.8% (pH 10.7, I = 14 mM), respectively. The coverage for high ionic strength samples is substantially higher: 44.6 ± 11.0% (pH 2.7, I = 100 mM), 99.8 ± 0.2% (pH 7.8, I = 100 mM) and 57.8 ± 1.7% (pH 11.5, I = 100 mM) for Fig. 6d–f. The AFM data are in line with the results from the FTIR measurements, as the corresponding coverage obtained from the conversion is 17.2% (pH 4.2, I = 14 mM), 46.4% (pH 7.8, I = 14 mM), 11.6% (pH 10.7, I = 14 mM), 55.8% (pH 2.7, I = 100 mM), 93.2% (pH 7.8, I = 100 mM) and 65.2% (pH 11.5, I = 100 mM).

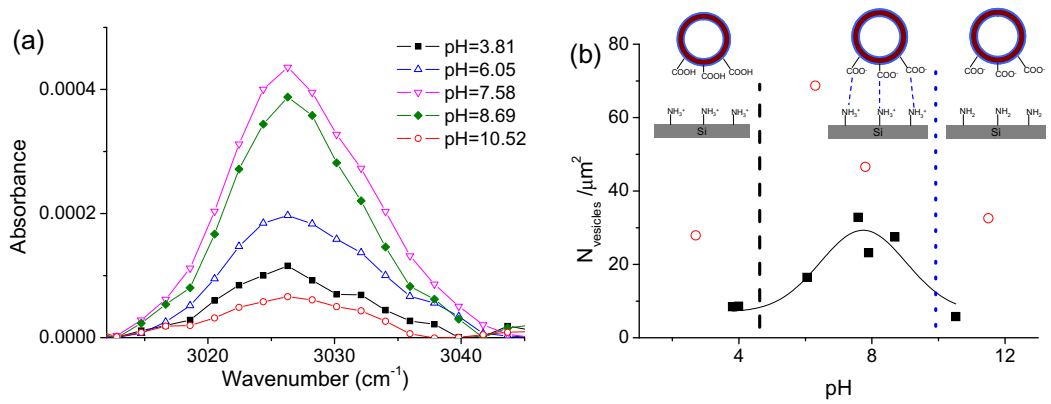

Fig. 5. Influence of pH on the immobilization of PS-*b*-PAA vesicles on NH_2-terminated silicon substrates. The absorbance at 3026 cm^{-1} in the FTIR spectra of PS-*b*-PAA vesicles deposited on NH_2-terminated silicon substrates from solutions with different pH values (I = 14 mM) is shown in (a), integrated and plotted in (b) as a function of pH (Squares). Another set of experiments with higher ionic strength (100 mM) is also shown (circles). The pK_a value of acrylic acid and primary amine are highlighted by a dashed line and a dotted line, respectively.

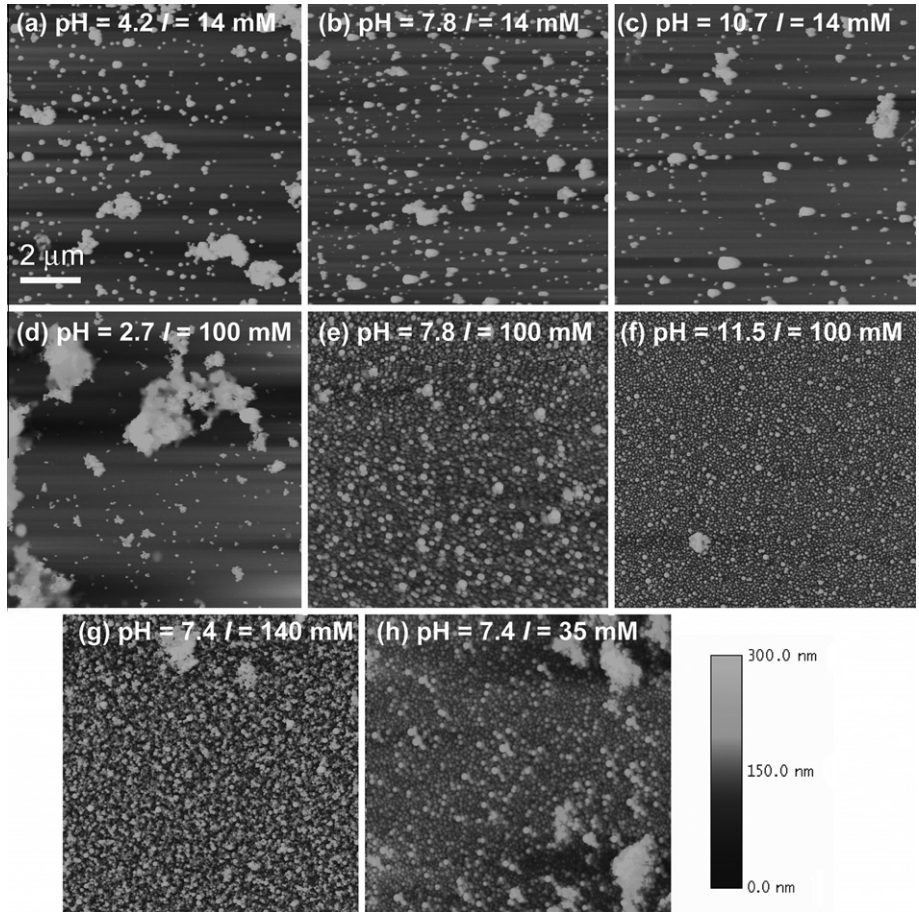

Fig. 6. TM-AFM images (scan size 10 μm × 10 μm) of PS-*b*-PAA vesicles immobilized onto NH_2-terminated silicon surfaces at different pHs and ionic strengths indicated in the legend.

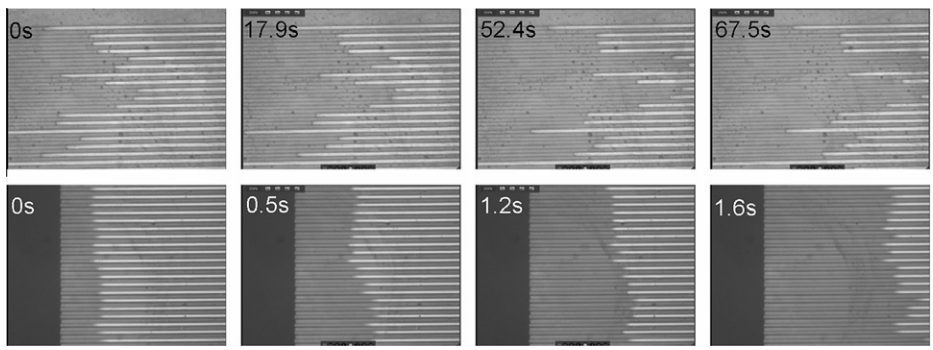

Fig. 7. Snapshots of the filling of the PDMS channel using PS-*b*-PAA vesicles in the presence or in the absence of salt. Upper row: No salt, filling speed 8.1 ± 0.8 μm/s. Lower row: NaCl concentration 35 mM, filling speed 478 ± 29 μm/s.

3.4. Patterning of PS-b-PAA vesicles on surfaces using MIMIC

To realize patterns of surface-attached vesicles, the immobilization of the vesicle nanoreactors was spatially confined using MIMIC [16]. In our experiments the surface of a polydimethylsiloxane (PDMS) mold was first oxidized by a UV-ozone treatment [33]. Channels were obtained by placing the mold on the surface of a substrate such that conformal contact with the surface was established. The relief structure in the mold in the form of an array of empty channels was filled by placing a droplet of vesicle solution at the open ends of the channels. The liquid spontaneously filled the channels by capillary action (Fig. 7). It was observed that the solution in the absence or in the presence

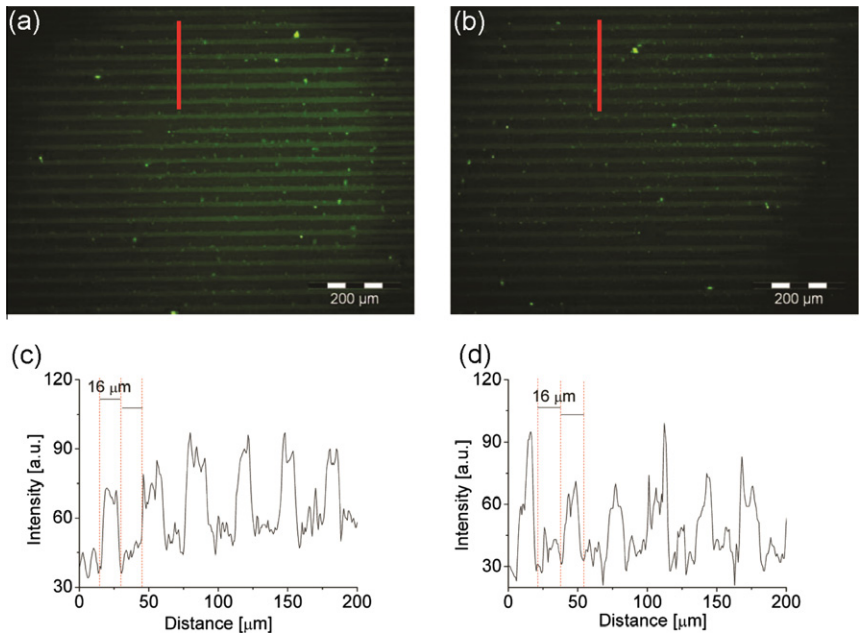

Fig. 8. Fluorescence microscopy images of line patterns of PS-*b*-PAA nanoreactors preloaded with enzymes and substrates deposited on NH_2-terminated glass substrate using MIMIC technique acquired (a) after the solvent was evaporated and (b) after rinsing extensively with Milli-Q water. (c) and (d) represent the cross-sectional intensity profiles of the fluorescence image as indicated by the lines in (a) and (b).

of salt filled the channels with substantially different speeds, which is attributed to the change in surface tension of the solution when salt is added [16] and a change in interfacial free energy due to the differences in surface coverage of immobilized vesicles (see above).

Similarly the channels were filled with PS-*b*-PAA vesicles containing R110-Arg_2 and trypsin. After the solution was dried, the stamp was removed from the surface and the glass substrate was rinsed extensively with pure water to remove only loosely bound vesicles. The line patterns created using MIMIC were investigated before and after the rinsing by fluorescence microscopy (Fig. 8). The fluorescence emission originated from R110 as the product of trypsin catalyzed hydrolysis reaction *inside* the vesicle nanoreactors.

No substantial loss of fluorescence intensity was observed when comparing the images before (Fig. 8a) and after (Fig. 8b) extensive rinsing, indicating that the vesicles were firmly immobilized onto the surfaces via electrostatic interactions and remained intact. Cross-sectional analyses of the images (Fig. 8c and d) showed that the dimensions of the patterns faithfully obeyed the dimensions of the channels fabricated with PDMS mold used (channel width 16 μm, separation 16 μm).

The successful filling of PS-*b*-PAA vesicles containing functional molecules using MIMIC and creation of line patterns of these vesicles provided us with a pathway to selectively immobilize miniature reaction vessels on solid supports which may find future applications in the real-time observation of reaction kinetics and dynamic behavior of biomolecules of interest. Future studies could be focused on the optimization and further miniaturization of the patterns, introduction of multiple functional vessels and integration of different functional subunits for the realization of a microarray system.

4. Conclusion

PS-*b*-PAA vesicles were immobilized onto solid surfaces functionalized with amino groups by means of electrostatic interactions, as was confirmed in experiments at various pH and ionic strength of the solution used for the immobilization. The vesicles were found to have a higher affinity to the surface at neutral pH as electrostatic interactions were minimized at both low and high pH. Higher ionic strength of the solution resulted in a larger number of vesicles deposited due to the screening of the electrostatic repulsion. The combination of MIMIC and the electrostatic immobilization strategy afforded line patterns of PS-*b*-PAA vesicles containing the enzyme trypsin and its substrate rhodamine 110 arginine bisamide. This demonstrated immobilization of functional nanoreactors highlights the feasibility for dynamic studies of enzymatic reactions inside individual nanoreactors immobilized onto surfaces and a potential means for the fabrication of vesicle-based microarray systems.

Acknowledgements

The authors are indebted to Professor Dr. R.G.H. Lammertink for the generous gift of the PDMS molds and gratefully acknowledge financial support of the MESA+

Institute for Nanotechnology of the University of Twente (SRO Bionanotechnology).

References

[1] Bally M, Halter M, Vörös J, Grandin HM. Optical microarray biosensing techniques. Surf Interface Anal 2006;38:1442–58.
[2] Howbrook DN, van der Valk AM, O'Shaughnessy MC, Sarker DK, Barker SC, Lloyd AW. Developments in microarray technologies. Drug Discovery Today 2003;8:642–51.
[3] Discher DE, Eisenberg A. Polymer vesicles. Science 2002;297:967–73.
[4] Yang JE, Gao CY. Progress in fabricating arrays of soft spherical vessels on mesoscale with spatial control. Chin Sci Bull 2008;53:3477–90.
[5] Kodadek T. Protein microarrays: prospects and problems. Chem Biol 2001;8:105–15.
[6] Zhu H, Snyder M. Protein chip technology. Curr Opin Chem Biol 2003;7:55–63.
[7] Jelinek R, Kolusheva S. Polymerized lipid vesicles as colorimetric biosensors for biotechnological applications. Biotechnol Adv 2001;19:109–18.
[8] Cooper MA. Advances in membrane receptor screening and analysis. J Mol Recognit 2004;17:286–315.
[9] Tresset G, Takeuchi S. Utilization of cell-sized lipid containers for nanostructure and macromolecule handling in microfabricated devices. Anal Chem 2005;77:2795–801.
[10] Antipov A, Shchukin D, Fedutik Y, Zanaveskina I, Klechkovskaya V, Sukhorukov G, et al. Urease-catalyzed carbonate precipitation inside the restricted volume of polyelectrolyte capsules. Macromol Rapid Commun 2003;24:274–7.
[11] Bolinger PY, Stamou D, Vogel H. Integrated nanoreactor systems: triggering the release and mixing of compounds inside single vesicles. J Am Chem Soc 2004;126:8594–5.
[12] Li F, Ketelaar T, Stuart MAC, Sudholter EJR, Leermakers FAM, Marcelis ATM. Gentle immobilization of nonionic polymersomes on solid substrates. Langmuir 2008;24:76–82.
[13] Li F, Ketelaar T, Marcelis ATM, Leermakers FAM, Stuart MAC, Sudholter EJR. Stabilization of polymersome vesicles by an interpenetrating polymer network. Macromolecules 2007;40:329–33.
[14] Stamou D, Duschl C, Delamarche E, Vogel H. Self-assembled microarrays of attoliter molecular vessels. Angew Chem Int Ed 2003;42:5580–3.
[15] Bolinger PY, Stamou D, Vogel H. An integrated self-assembled nanofluidic system for controlled biological chemistries. Angew Chem Int Ed 2008;47:5544–9.
[16] Xia YN, Whitesides GM. Soft lithography. Angew Chem Int Ed 1998;37:551–75.
[17] Mahajan N, Lu RB, Wu ST, Fang JY. Patterning polymerized lipid vesicles with soft lithography. Langmuir 2005;21:3132–5.
[18] Baek JH, Ahn H, Yoon J, Kim JM. Micro-patterning of polydiacetylene supramolecules using micromolding in capillaries (MIMIC). Macromol Rapid Commun 2008;29:117–22.
[19] Ahn DJ, Kim JM. Fluorogenic polydiacetylene supramolecules: immobilization, micropatterning, and application to label-free chemosensors. Acc Chem Res 2008;41:805–16.
[20] Chen Q, Schönherr H, Vancso GJ. Block copolymer vesicles as nanosized reactors for enzymatic reactions. Small 2009;5:1436–45.
[21] Chen Q, Rausch KG, Schönherr H, Vancso GJ. α-Chymotrypsin catalyzed reaction confined in block copolymer vesicles. ChemPhysChem 2010;11:3534–40.
[22] Vriezema DM, Garcia PML, Oltra NS, Hatzakis NS, Kuiper SM, Nolte RJM, et al. Positional assembly of enzymes in polymersome nanoreactors for cascade reactions. Angew Chem Int Ed 2007;46:7378–82.
[23] Cisse I, Okumus B, Joo C, Ha T. Fueling protein–DNA interactions inside porous nanocontainers. Proc Natl Acad Sci USA 2007;104:12646–50.
[24] Provencher SW. Fourier method for analysis of exponential decay curves. Biophys. J. 1976;16:27–41.
[25] Chen Q, Schönherr H, Vancso GJ. Encapsulation and release of molecular cargos via temperature induced vesicle-micelle transition. Small. doi:10.1002/smll.201001348.
[26] Vibration bands: for PS: ν(CH) aromatic 3083, 3060, 3026 cm^{-1}, $\nu_{as}(CH_2)$ 2924 cm^{-1}, $\nu_s(CH_2)$ 2860 cm^{-1}, ν(C–C)aromatic 1493, 1453 cm^{-1}; for PAA: $\nu_{as}(CH_2)$ 2926 cm^{-1}, $\nu_s(CH_2)$ 2852 cm^{-1}, ν(C=O) 1710 cm^{-1}.
[27] Chauhan AK, Aswal DK, Koiry SP, Gupta SK, Yakhmi JV, Sürgers C, et al. Self-assembly of the 3-aminopropyltrimetoxysilan multilayers on Si and hysteretic current-voltage characteristics. Appl Phys A Mater 2008;90:581–9.
[28] Kosmulski M. Chemical properties of material surfaces. New York: Marcel Dekker; 2001.
[29] The conversion of PS-*b*-PAA film thickness (d) to the number of vesicles ($N_{vesicles}$) per μm^2 was done assuming the coverage of vesicles is homogeneous on the surface and the vesicles have a monomodal size distribution with a radius of $R = 75$ nm and a membrane thickness of $t = 25$ nm. The PS volume (V_{PS}) for an individual vesicle is expressed by the following equation: $V_{PS} = 4/3\pi R^3 - 4/3\pi(R-t)^3$. The total volume of PS is kept constant, which equals the PS volume for an individual vesicle multiplied by the number of vesicles per unit area ($A = 1\ \mu m^2$ is used for the simplicity of calculation), as well as the thickness of the film multiplied by the area of the film: $V_{total\ PS} = N_{vesicles} \cdot V_{PS} = d \cdot A$.
[30] Brandrup J, Immergut EH. Polymer handbook. New York: John Wiley and Sons; 1989.
[31] Russel WB, Saville DA, Schowalter WR. Colloidal dispersions. Cambridge: Cambridge University Press; 1989.
[32] Ise N, Sogami IS. Structure formation in solution: ionic polymers and colloidal particles. Berlin/Heidelberg/New York: Springer; 2005.
[33] Hillborg H, Tomczak N, Olàh A, Schönherr H, Vancso GJ. Nanoscale hydrophobic recovery: a chemical force microscopy study of UV/ozone – treated crosslinked poly(dimethylsiloxane). Langmuir 2004;20:785–94.